A Numerical Study of Viscosity Effects on the Breakup of Shear-Dependent Droplet in Microfluidics Using Level-Set Method

Voon-Loong Wong*[1], Kar-Hing Yau[1], Katerina Loizou[2], Phei-Li Lau[3], Richard S. Graham[2], and Buddhika N. Hewakandamby[2]
[1] Faculty of Engineering and the Built Environment, SEGi University, Kota Damansara, Petaling Jaya 47810, Selangor Darul Ehsan, Malaysia.
[2] University of Nottingham, Nottingham NG7 2RD, United Kingdom.
[3] University of Nottingham Malaysia Campus, Semenyih 43500, Malaysia.
*Corresponding author: wongvoonloong@segi.edu.my

Abstract: This paper presents the parametric studies of the effect of viscosity on breakup dynamics of the non-Newtonian sodium carboxymethylcellulose (CMC) microdroplets. Numerical studies are performed on the fluid dynamics of CMC droplets with shear-thinning properties in an immiscible liquid-liquid system. Properties of the dispersed phase simulated has a range of viscosities similar to that of aqueous solutions comprising of 0.02 wt% to 1.20 wt% CMC in an oil phase that serves as the continuous phase in a microfluidic T-junction. A Carreau-Yasuda stress model is incorporated with a two-phase conservative Level-Set (LS) method to capture the droplet breakup dynamics and relevant hydrodynamics. The numerical simulations predicted that the viscosity effect of both phases has a major influence on controlling the diameter of the trains of CMC droplets in microfluidic flow. These findings will provide explicit information on the impact of rheological behaviour of the microdroplets.

Keywords: Non-Newtonian, Carreau-Yasuda, Microfluidics, COMSOL Multiphysics.

1. Introduction

Microfluidic systems have been established as an alternative and versatile platform for microdroplets formation in many scientific fields such as biology, medical, chemical, and drug discovery. Prior experimental [1, 2] and numerical [3, 4] studies have considered mostly Newtonian fluids and their importance in the field of microfluidics. Nevertheless, most real fluids used in lab-on-chip devices in industrial practice exhibit non-Newtonian behaviour. Unlike Newtonian fluids that obey Newton's law of viscosity, non-Newtonian fluids act differently. Many non-Newtonian fluids have flow characteristics that do not conform to a linear relationship between shear stress and shear rate in simple shear. Moreover, there is no single constitutive equation established to describe the rheogram of all such fluids. Previously, most published studies have been reported in the area of empirical studies on the effect of viscoelasticity and molecular weight on elastic and viscous droplet breakup process [5, 6].

Existing studies of Newtonian droplets breakup have focused mainly on the role of the viscosity for the control of droplet size in emulsification process. These results revealed that viscosity of the liquid phase is one of the leverage factors influencing the motion and shape evolution of droplets in microfluidic flow. However, a detailed empirical or numerical study of viscosity effect on the non-Newtonian system has not been examined previously. Garteski *et al*. [1] characterize the role of the viscosity on droplet size variation in order to test the postulated shear-dominated scaling relation. Besides, Christopher *et al*. [7] experimentally found that droplet size is weakly dependent on viscosity ratio, with the exception of the largest ratio (λ = 1/6). Gupta and Kumar [3] numerically predicted that the viscosity of continuous phase markedly influences the droplet volume for different flow regimes. Fu *et al*. [8] reported that the droplet diameter can be scaled as power-law relation with the exponent dependent on the viscosity ratio for jetting regime. To our best knowledge, there is little information about the viscosity effect on the formation of non-Newtonian droplets in microfluidics device.

Prior to any forthcoming experimental works, a highly reliable numerical method is essential to forecast the performance of a module in terms of functionality of the entire system. Microdroplets formation is a process involving moving boundaries and interfaces. The interface geometry is usually complex and it can undergo large deformations or even topology changes of

interface. Interface tracking [9, 10] and interface capturing [11, 12] are two main approaches to represent the interface evolution problem to the Navier-Stokes equation discretized on a fixed grid. Interface tracking approaches based on explicit description of the interface by the computational mesh provide great accuracy; however, their applicability is limited in the case of severe interface motion. On the contrary, the interface motion can be simply obtained by the advection of the corresponding phase function in interface capturing (implicit) method. Level-set method is one of the interface capturing methods which has become a usual way to localize the interface. The major drawback of the classical LS method is that mass is not conserved, hence leading to significant mass losses. In attempts to improve the mass conservative properties of the classical LS method, Olsson and Kreiss [13] have proposed a conservative LS method which has resolved the mass conservation issues associated with numerical scheme and thus possesses high order accuracy for the modelling of multiphase flow. This method is very computationally intensive, but it is relatively simple to code [13].

In present theoretical analysis, the effects of continuous and dispersed phase viscosity in tailoring the droplet size were numerically investigated. A numerical model was proposed and developed to predict the droplet size and uniformity as a function of fluid viscosity with the application of conservative LS method used in a CFD computation. Non-Newtonian CMC is selected as the material which exhibits the shear-thinning rheological behaviour. The processes of droplet generation were preliminarily investigated using CMC as dispersed phase and different type of Newtonian oils as the continuous phase in microfluidic device with T-shaped geometry. Current parametric numerical investigation of fluid viscosity effect can be established as the conceptual framework of non-Newtonian droplet generation process and relevant phenomena for future empirical studies.

2. Mathematical Model and Numerical Algorithm

A conservative LS method that was proposed by Olsson and Kreiss [13] was employed to track the fluid-fluid interface in present study. The interface between two immiscible fluids is considered to be sharp and characterized by the 0.5 contour of the LS function (ϕ=0.5). A T-shaped model with dimension of 220 µm (w_c) × 90 µm (w_d) in present simulation is illustrated in Fig.1. The main channel is filled with the continuous phase (ϕ=0) and the dispersed phase (ϕ=1) is placed in the lateral channel. The following equations (Eq. (1)-(9)), which defines the LS method, were solved by standard finite element methods. This was achieved using COMSOL's implementation of the LS method from CFD module.

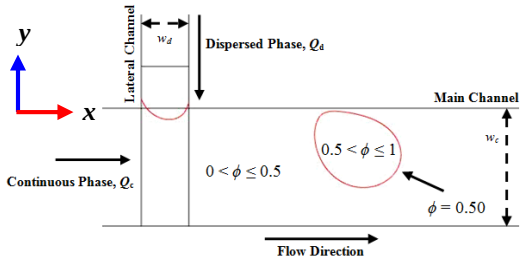

Figure 1. Contour representation of interface location for a droplet generated.

The fluid interface uses the following equation (Eq. (1)) described the convection of reinitialized LS function:

$$\frac{\partial \phi}{\partial t} + \mathbf{u} \cdot \nabla \phi = \gamma \nabla \left[\varepsilon \nabla \phi - \phi(1-\phi) \frac{\nabla \phi}{|\nabla \phi|} \right] \quad (1)$$

Eq. (1) is coupled to the governing equations consisting of the incompressible Navier-Stokes equation (Eq. (2)) and continuity equation (Eq. (3)) for the advection of LS function:

$$\rho \frac{\partial \mathbf{u}}{\partial t} + \rho(\mathbf{u} \cdot \nabla)\mathbf{u} = \nabla \left[-pI + \eta(\nabla \mathbf{u} + (\nabla \mathbf{u})^T \right] + F_{st} \quad (2)$$

$$\nabla \cdot \mathbf{u} = 0 \quad (3)$$

The F_{st} term acting on the interface between two fluid phases can be determined by Eq. (4):

$$F_{st} = \sigma k \mathbf{n}_\Gamma \delta_{sm} \quad (4)$$

where the local interfacial curvature (k), the unit normal vector ($\mathbf{n}_\Gamma$), and the smeared out Dirac delta function (δ_{sm}) can be defined as:

$$k = -\nabla \cdot \mathbf{n}_\Gamma \quad (5)$$

$$\mathbf{n}_\Gamma = \frac{\nabla \phi}{|\nabla \phi|} \quad (6)$$

$$\delta_{sm} = 6|\phi(1-\phi)||\nabla \phi| \quad (7)$$

In simulating two-phase flows, the fluid properties of density and the dynamic viscosity across the interface are calculated from Eq. (8) and Eq. (9), respectively:

$$\rho = \rho_1 + (\rho_2 - \rho_1)\phi \quad (8)$$

$$\eta = \eta_1 + (\eta_2 - \eta_1)\phi \quad (9)$$

where ρ_1 and ρ_2 are the densities of the continuous phase and dispersed phase, η_1 and η_2 are the viscosities of continuous phase and dispersed phase respectively.

In present work, all the parametric studies used as key output the effective droplet diameter (d_{eff}). An integration operator was added to find the area corresponding to the dispersed phase, where $\phi > 0.5$, in order to calculate the effective droplet diameter by following equation:

$$d_{eff} = 2 \cdot \sqrt{\frac{1}{\pi} \int_{\Omega} (\phi > 0.5) d\Omega} \quad (10)$$

3. Results and Discussion

Based on the proposed predictive model over a previous validation [14], a set of numerical parameters have been selected. In present model, an optimal grid resolution containing 7644 mapped mesh elements was adopted. Simulations were performed at a time step of 0.0005 s and constant Q of 0.05 (Q_c = 2.0 ml/h, Q_d = 0.1 ml/h). A contact angle of 180° that represents the complete repulsion of working liquid by the channel wall surface was applied in the computation. In present study, the continuous phase was modelled as a Newtonian fluid, whereas the dispersed phase was modelled by the Carreau-Yasuda model, with model parameter chosen to fit linear rheological measurements on a CMC solution at a range of concentrations (see *Appendix A*).

3.1 Effect of dispersed phase concentration

The present study was designed to determine the influence of CMC concentration (0.02 wt% to 1.20 wt%) on generated droplet size and the results of prediction data are illustrated in Fig. 2. Olive oil (η_c = 0.068 kg/m s) was selected as the carrier fluid in continuous phase along the main channel. The results revealed that the larger concentration of CMC dispersed fluid results in significant effects on reducing the size of generated droplets. Viscosity of a polymer solution depends on its concentration and molecular weight of the dissolved polymer. When the CMC liquid is more viscous, the viscous pressure in dispersed thread becomes more dominant. Davidson and Cooper-White [15] reported that the larger effect of shear-thinning will tend to reduce the resulting droplet length for higher viscosity. Theoretical predictions of the viscosity effect on droplet diameter are found dissimilar to the previous studies for dispersed fluid with different non-Newtonian properties. Husny and Cooper-White [5] reported that larger droplet was produced for solutions containing higher polyethylene oxide molecular weights and viscosity. Similar empirical observation to the viscoelastic fluid was also observed by Steinhaus and Shen [16]. Gu and Liow [17] has also observed that larger diameter drops were produced for larger viscosity of shear-thinning xanthan gum solution. Non-Newtonian fluids always display a host of flow instabilities and even exacerbate the instabilities in different microfluidic configuration. Thus, dissimilar phenomena may be accounted due to the complexity of non-Newtonian flow behaviour.

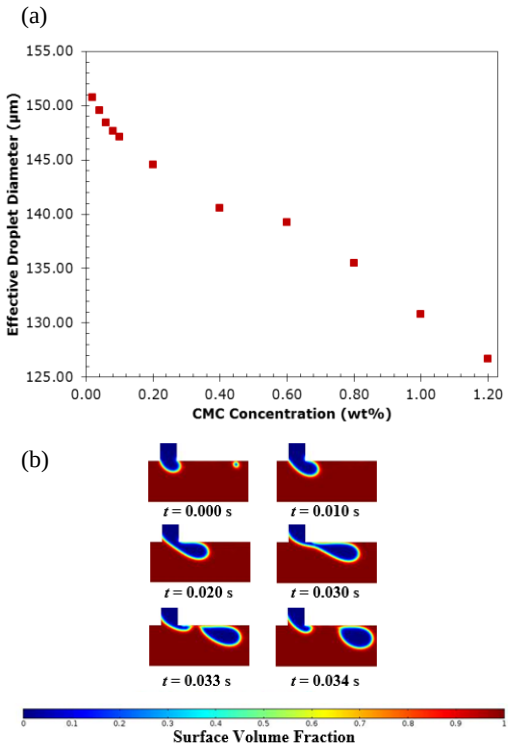

Figure 2. Illustrations of (a) effect of CMC concentration on effective droplet diameter and (b) the snapshots of droplet breakup process of 0.40 wt% CMC.

3.2 Effect of continuous phase viscosity

This study set out with the aim of examining the role of the η_c on CMC droplets in the context of droplet size distribution at each CMC concentrations and these results are plotted graphically in Fig. 3(a). Three different viscosities, 0.00354 kg/m s (mineral oil), 0.068 kg/m s (olive oil), and 0.0988 kg/m s (peanut oil) of continuous phase (from data in [18]) were employed for current studies. The prediction revealed that droplet diameter decreases as η_c increases.

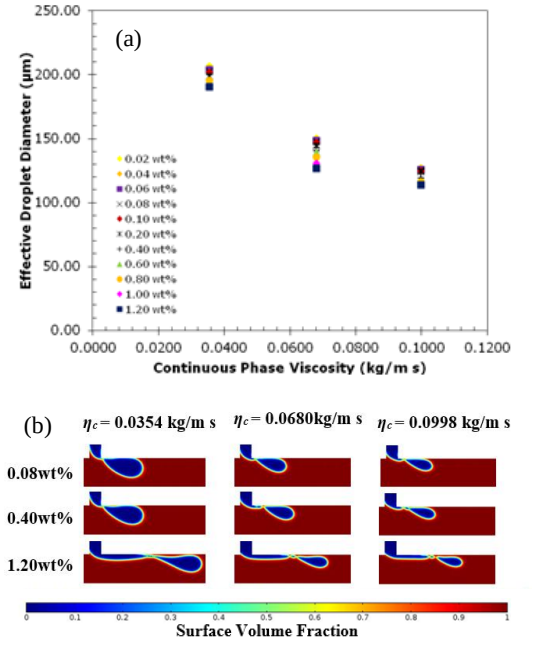

Figure 3. Illustration of (a) the effect of η_c on effective droplet diameter of CMC droplets and (b) snapshots of the effect of η_c on flow pattern at different CMC concentrations.

Increasing the η_c generally give rise to increasing shear force on penetrating dispersed phase thread and thus a higher likelihood of leading to less stable thread. Therefore, smaller droplets are being generated. These findings are consistent with those earlier experimental studies [17, 19]. Nevertheless, it differs from previous findings [3], which stated that the droplet volume is increased with increasing η_c. Prior studies [20] have noted that the volume (relative to droplet size) of a final droplet at the end of the growth and detachment stages is determined by the forces balance at the detachment point. The droplet is generated when the equilibrium of forces is achieved. Surface tension force, shear-stress force, and resistance force are the dominant forces that generally act on the emerging tip of dispersed thread as reported by Garteski *et al*. [1]. At lower η_c, viscous shear-stress appear to be minimised and surface tension (mineral oil, 41.37 mN/m> olive oil, 20.74 mN/m> peanut oil, 18.80 mN/m, from data in [19]) becomes increasingly dominant on the breakup process. While increasing η_c, shear-stress force exerted on the interface by continuous phase could largely increase. The flow pattern map for perpendicular inlet of CMC dispersed phase configuration is shown in Fig. 3(b). As seen in Fig. 3(b), the larger η_c (corresponding to a larger drag force) will force the position of CMC droplet detachment point to move further to the downstream from T-junction before droplets are being sheared off in the main channel, resulting in generation of smaller droplets.

3.3 Effect of fixed dispersed to continuous phase viscosity ratio

Present study investigating the combined effects of both phases on the droplet diameter have primarily focused on changing the η_c in order to achieve a constant λ ($=\eta_o/\eta_c$) of 1 at each CMC concentration ranging from 0.04 wt% to 0.4 wt% (where $0.0121<\eta_o<0.1946$ kg/m s, see Table A-1). The η_c is varied with the value which is equivalent to the zero shear viscosity (η_o) for each CMC concentration, as listed in Table A-1 (*Appendix A*) in CMC solution, coupled with its shear-thinning character. The η_o corresponds to the dispersed phase fluid which is completely structured without any disruption at the very low shear. Fig. 4 illustrates the plot of the effects of similar viscosities of both phases on the droplet diameter of CMC solutions. By considering the aforementioned state with λ=1, the resulting droplet diameter decreases as similar viscosities of both phases increases. According to the shear-thinning behaviour of CMC, the η_d decreases with the rate of the shear strain. Moreover, the greater the η_o for higher concentration, the more dispersed particles or colloids present in the fluid system. The larger intermolecular friction between particles may induce more resistance to flow results in less flow. Under high shear rates in microfluidic device, the continuous phase with the identical value of η_o always dominates the

droplet breakup process due to the fact that η_c is constantly larger than the averaged η_d. When $\eta_c >> \eta_d$, the viscous shear stress induced by the continuous phase, which is a vital distorting force acting on interface, becomes prevailing. As the η_c effect becomes greater, the results revealed that the neck of droplets drains more rapidly as the pressure acting along the neck of the dispersed threads increases. This will tend to accelerate the droplet breakup process resulting in the formation of smaller droplets. These findings are found to be consistent with those in available studies [21, 22].

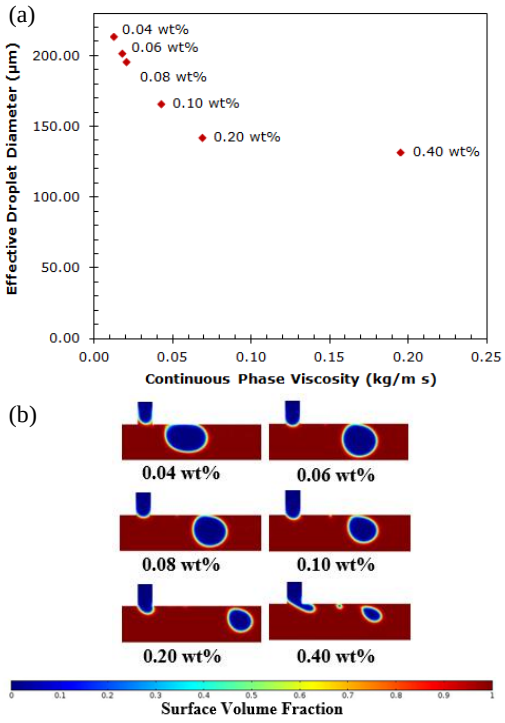

Figure 4. Illustration of (a) the effect of fixed η_o/η_c on CMC droplets breakup diameter and (b) snapshots of the effect of fixed η_o/η_c on flow pattern at different CMC concentrations.

4. Conclusions

A two-phase conservative LS approach effectively captured the dynamics and relevant hydrodynamics of droplet breakup process in a microfluidics T-junction with the prescribed geometry size. Shear-thinning CMC was selected as dispersed phase, while different Newtonian oil types were selected as continuous phase. The fluid of interest, CMC solution with concentrations ranging from 0.02 wt% to 1.20 wt%, is a purely viscous fluid obeying the Carreau-Yasuda model in order to examine the effect of shear-thinning on breakup process. Some concluding observations from the parametric analysis are given below:

- Varying CMC concentrations: Effective droplet diameters decrease as concentration increases. Nevertheless, theoretical predictions are found to be inconsistent to those previous empirical observations that focused on dispersed fluid with different non-Newtonian characteristic.
- Varying η_c: Three different types of continuous phase with different viscosities classes were employed. Larger η_c was expected to induce higher viscous shearing force acts on penetrating dispersed phase thread, thus reducing the droplet diameter. This effect was seen in our calculations.
- Fixed η_o/η_c: Considering a fixed λ of 1, the η_c is varied with equivalent to the CMC concentration dependence of η_o in CMC solution. The resultant droplet diameter is markedly decreased by increasing the equivalent viscosity of both phases.

5. References

[1] Garstecki, P.; Fuerstman, M.J.; Stone, H.A.; and Whitesides, G.M. Formation of droplets and bubbles in a microfluidic T-junction-scaling and mechanism of breakup. *Lab Chip*, **6**, 437-446 (2006)

[2] Xu, J.H.; Luo, G.S.; Li, S.W.; and Chen, G.G. Shear force induced monodisperse droplet formation in a microfluidic device by controlling wetting properties. *Lab on a Chip*, **6**, 131-136 (2006)

[3] Gupta, A.; and Kumar, R. Flow regime transition at high capillary numbers in a microfluidic T-junction: Viscosity contrast and geometry effect. *Physics of Fluids*, **22**, 122001, 1-11 (2010)

[4] Glawdel, T.; Elbuken, C.; and Ren, C.L. Droplet formation in microfluidic T-junction generators operating in the transitional regime. II. Modelling. *Physical Review*, **85**, 016323-1-016323-12 (2012)

[5] Husny, J.; and Cooper-White, J.J. The effect of elasticity on drop creation in T-shaped microchannels. *Journal of Non-Newtonian Fluid Mechanics*, **137**, 121-136 (2006)

[6] Arratia, P.E.; Cramer, L.A.; Gollub, J.P.; and Durian, D.J. The effects of polymer molecular weight on filament thinning and drop breakup in

microchannels. *New Journal of Physics*, **11**, 115006, 1-18 (2009)
[7] Christopher, G.F.; Noharuddin, N.N.; Taylor, J.A.; and Anna, S.L. Experimental observations of the squeezing-to-dripping transition in T-shaped microfluidic junctions. *Physical Review*, **78**, 036317, 1-12 (2008)
[8] Fu, T.T.; Wu, Y.N.; Ma, Y.G.; and Li, H.Z. Droplet formation and breakup dynamics in microfluidic flow focusing devices: From dripping to jetting. *Chemical Engineering Science*, **84**, 207-217 (2012)
[9] Hou, T.Y.; Lowengrub, J.S.; and Shelley, M.J. Boundary integral methods for multicomponent fluids and multiphase materials. *Journal of Computational Physics*, **169**, 302-362 (2001)
[10] Tryggvason, G.; Bunner, B.; Esmaeeli, A.; Juric, D.; Al-Rawahi, N.; Tauber, W.; and Jan, Y. J. A front-tracking method for the computations of multiphase flow. *Journal of Computational Physics*, **169(2)**, 708-759 (2001)
[11] Takada, N.; Misawa, M.; Tomiyama, A.; and Fujiwara, S. Numerical simulation of two- and three-dimensional two phase fluid motion by Lattice Boltzmann method. *Computer Physics Communications*, **129**, 233- 246 (2000)
[12] Osher, S.; and Sethian, J.A. Fronts propagating with curvature-dependent speed: algorithms based on Hamilton-Jacobi formulations. *Journal of Computational Physics*, **79**, 12-49 (1988)
[13] Olsson, E.; and Kreiss, G. A conservative level set method for two phase flow. *Journal of Computational Physics*, **210**, 225-246 (2005)
[14] Wong, V.L.; Loizou, K.; Lau, P.L.; Graham, R.S.; and Hewakandamby, B.N. *Numerical simulations of the effect of rheological parameters on shear-thinning droplet formation*. Proceedings of the ASME 4th Joint US-European Fluids Engineering Division Summer Meeting, Chicago, Illinois, August 3-8, 9pp (2014)
[15] Davidson, M.R., and Cooper-White, J.J. Pendant drop formation of shear-thinning and yield stress fluids. Applied Mathematics Modelling, **30**, 1392–1405 (2006)
[16] Steinhaus, B.; and Shen, A.Q. Dynamics of viscoelastic fluid filaments in microfluidic devices. *Physics of Fluids*, **18**, 073103, 1-13 (2007)
[17] Gu, Z.P.; and Liow, J.L. Microdroplet formation in a T-junction with xanthan gum solutions. *Chemeca: Australasian Conference on Chemical Engineering* (2011)
[18] Loizou, K.; Wong, V.L.; Thielemans, W.; and Hewakandamby, B.N. *Effect of Fluid Properties on Droplet Generation in a Microfluidic T-junction*. Proceedings of the ASME 4th Joint US-European Fluids Engineering Division Summer Meeting, Chicago, Illinois, August 3-8, 9pp (2014)
[19] Yeom, S.; and Lee, S. Y. Size prediction of drops formed by dripping at a micro T-junction in liquid–liquid mixing. *Experimental Thermal and Fluid Science*, **35**, 2, 387-394 (2011)
[20] Husny, J., Jin, H.Y., Harvey, E., and Cooper-White, J.J. Dynamics of shear-induced drop formation in T-shaped microchannels. *Seventh International Conference on Miniaturized Chemical and Biochemical Analysts Systems*, **1**, 113-116 (2003)
[21] Liu, H.; and Zhang, Y. Droplet formation in T-shaped microfluidic junction. *Journal of Applied Physics*, **106**, 034906, 1-8 (2009)
[22] Bashir, S.; Rees, J.M.; and Zimmerman, W.B. Simulations of microfluidics droplet formation using the two-phase level set method. *Chemical Engineering Science*, **66**, 4733-4741(2011)

6. Appendix

Table A-1: Carreau-Yasuda Model Constant Measure Data [14]

CMC (wt%)	Viscosity / Carreau-Yasuda Model Constant*				
	η_o (kg.m.s)	η_∞ (kg/m.s)	$\lambda(s)$	n	a
0.02	0.0070	0.0003	0.0400	0.7121	0.9653
0.04	0.0121	0.0000	0.0325	0.7102	1.6980
0.06	0.0171	0.0000	0.0256	0.6775	1.3728
0.08	0.0195	0.0028	0.0143	0.4886	1.1319
0.10	0.0420	0.0007	0.0572	0.6242	0.4734
0.20	0.0742	0.0006	0.0041	0.3528	0.3856
0.40	0.1946	0.0040	0.0138	0.3157	0.5534
0.60	0.7995	0.0022	0.0147	0.1995	0.3660
0.80	1.6469	0.0057	0.0515	0.2444	0.4782
1.00	4.1143	0.0031	0.1604	0.2869	0.5000
1.20	10.264	0.0000	0.2069	0.2297	0.4175

**Measurements were performed on controlled stress rheometer at 20°C. All data were fitted to Carreau-Yasuda model for all CMC concentrations*:

$$\frac{\eta-\eta_\infty}{\eta_0-\eta_\infty} = [1 + (\lambda_{CY}\dot{\gamma})^a]^{\frac{n-1}{a}} \quad \text{(A.1)}$$